

# Experimental Parameter Effect on Ceramic Coating Film on LY12 Alloy by Micro-arc Oxidation

H ZHAO<sup>1</sup>, J H YANG<sup>1</sup> and X H WANG<sup>2</sup>

<sup>1</sup> College of Materials Science and Engineering, Shenyang Ligong University, China

<sup>2</sup> College of Materials Science and Engineering, Shenyang University of Technology, China

E-mail: zhaohui\_1968@sina.com

**Abstract.** Ceramic coatings were fabricated on the surface of LY12 aluminum alloy by micro-arc oxidation (MAO) method in NaSiO<sub>3</sub>-NaOH solution. Effect of experimental parameter on the MAO film was investigated. The results show that the ceramic layers formed on the surface of the alloy show different surface morphologies, and thickness of MAO film increases with the increase of voltage and oxidation time. These films contain two layers, an outer porous layer and an inner barrier layer, which consists mainly of  $\gamma$ -Al<sub>2</sub>O<sub>3</sub> phase and a small amount of  $\alpha$ -Al<sub>2</sub>O<sub>3</sub> phase..

## 1. Introduction

A microarc oxidation (MAO) is a novel surface technique being wide used in depositing thick and ultra-hard ceramic coatings on valve metals substrate [1-3]. A key feature of the process is a plasma discharge that occurs at the metal/electrolyte interface when the applied voltage exceeds a certain critical breakdown value and appears as a number of discrete short-lived micro-discharges moving across the metal surface [4]. The MAO film has a lot of characteristics, such as high micro-hardness, high electric insulation resistance and good adhesion with the substrate [5].

Much Research has been focused on aluminum and aluminum alloys in recent years due to their low density, high specific strength and great machinability [6], but they are sometimes limited in applications because of their moderately poor corrosion resistance and tribological properties [7, 8]. Therefore, surface modification techniques of aluminum alloys, such as MAO, have been paid much attention. It is necessary to investigate the formation of ceramic film on aluminum alloy prepared by MAO.

MAO coatings were prepared on LY12 alloy by microarc oxidation in this study. Different experimental parameters, such as different voltage, different oxidation time, are employed. The microstructure, surface morphology and phase composition of MAO coatings on LY12 alloy under different conditions were analyzed in details.

## 2. Experimental

LY12 alloy plates in the size of 60×30×2 mm were used as the substrate. The MAO coatings were prepared by using pulse microarc oxidation system. The constant voltage mode was employed, and the constant pulse width and interval was selected as 500  $\mu$ s and 1000 s. An aqueous solution, comprising mainly NaSiO<sub>3</sub> (4g/L), NaOH (2g/L) and some other substances to adjust its alkalinity and increase electric conductivity, was used as the electrolyte. Stainless steel plate was used as a cathode while LY12 alloy specimen as an anode. The temperature of the solution was controlled below 25 °C and the



oxidation time is 15 min, 20 min and 25 min respectively. Different voltages (400V, 440 V, 480 V) were used respectively.

The thickness of the coatings was measured using a coating thickness gauge (TT230). SEM (HORIBA S-3400) was used to investigate the morphology of surface and the cross-section of the specimen. Rigaku Vltima IV diffractometer was used to investigate the phase constituent of the coatings.

### 3. Results and discussion

#### 3.1 Voltage effect on the MAO film of LY12 alloy

Figure 1 shows the surface morphologies of the MAO coatings on LY12 alloy under different voltages. When the coating is formed at lower voltage, the particles on the surface coatings are smaller, fine and uniform micro-pores distribute randomly on the surface (Fig. 1(a)). With the increase of voltage, MAO reaction become to be violent, more and larger oxide particles are produced. Therefore, the number of micro-pores decreases quickly, while the size of which increases significantly (Fig. 1(b)). Moreover, the surface of coatings is roughened with the increase of voltage. At this time, melting particles are deposited on the surface and obstruct the discharging channels as a result of much higher discharging energy induced by intense micro-arc discharging. At the voltage of 480 V, rough ceramic surface is formed and much more oxides are developed under higher breakdown voltage (Fig. 1(c)).

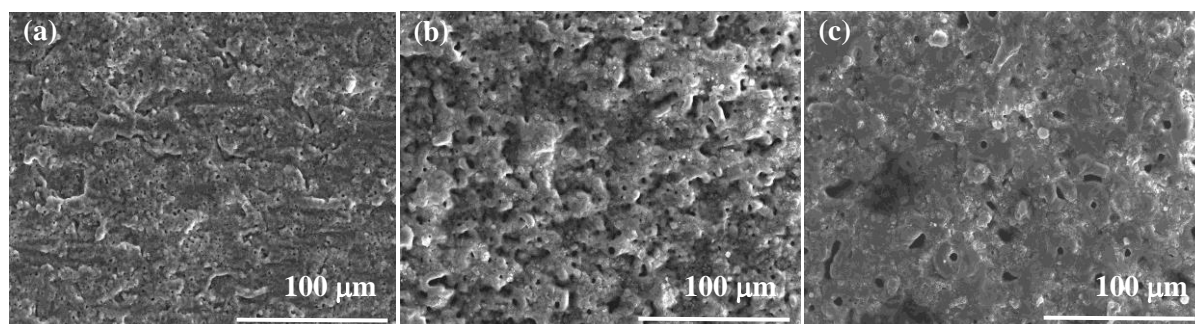


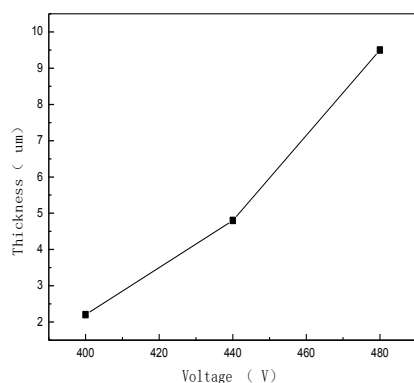
**Figure 1.** Surface morphologies of the ceramic coatings on LY12 alloy under different voltages. (a) 400 V, (b) 440 V, (c) 480 V.

The variation of the thickness of the MAO coatings on LY12 alloy is shown in Fig. 2 as a function of voltage. With an increasing voltage, the thickness of the coatings increases. An approximately linear growth of the coatings has been observed. The growth rate of the coatings is very fast, and the coating thickness goes up from about 2 to 10  $\mu\text{m}$ .

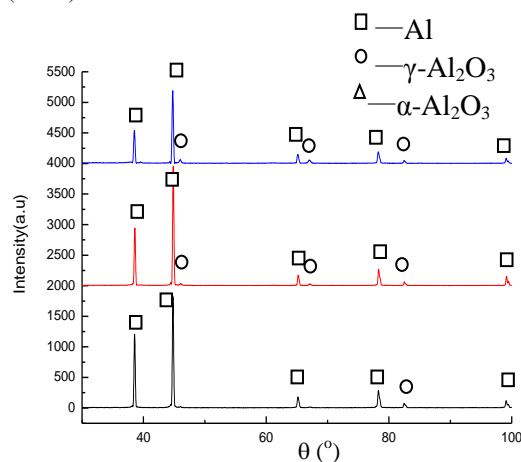
Figure 3 shows the XRD patterns of the coatings on LY12 alloy under different MAO voltages. It can be determined that the MAO coating is composed of  $\gamma\text{-Al}_2\text{O}_3$  mainly and a small amount of  $\alpha\text{-Al}_2\text{O}_3$ . With the increase of voltage, more and more aluminum hydrate anions accumulated at the interface between the alloy and the electrolyte. Aluminum substrate was transformed into  $\gamma\text{-Al}_2\text{O}_3$  and  $\alpha\text{-Al}_2\text{O}_3$ , and bright surface of aluminum alloy became to be dark. Therefore, XRD peaks show decreased aluminum phases and increased  $\gamma\text{-Al}_2\text{O}_3$  and  $\alpha\text{-Al}_2\text{O}_3$  phases with the increase of voltage.

#### 3.2 Oxidation time effect on the MAO film of LY12 alloy

Surface morphologies of the MAO coatings on LY12 alloy under different oxidation time were shown in Fig. 4. At the beginning, uniformly dispersed micro-discharging channels are easier to occur on the surface of alloy, so that the size of micro-pores is significantly small, and the coatings are compact. With an increasing oxidation time, the coatings are characterized by micro-pores with different sizes.

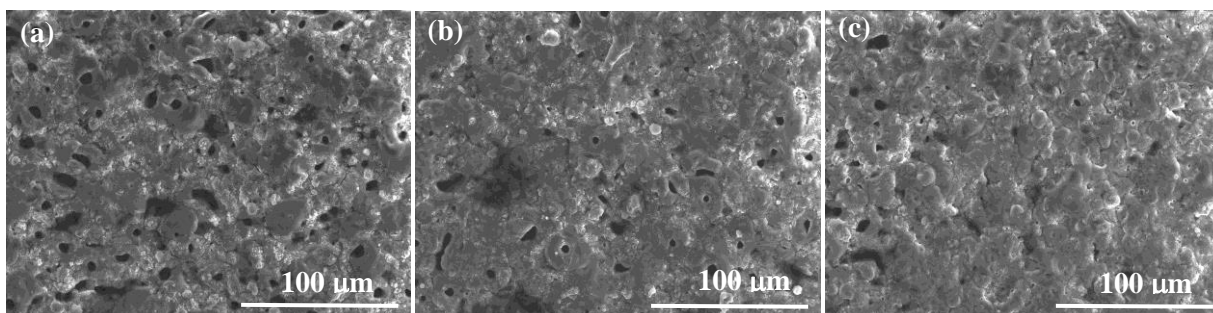


**Figure 2.** Variation of the thickness of MAO coatings on LY12 alloy with voltage.



**Figure 3.** XRD patterns of MAO coatings on LY12 alloy under the voltage of (a) 400 V, (b) 440 V, (c) 480 V

Enlarged micro-pores were observed, and the coatings become porous and loose, as shown in Figs. 4(a) and (b). The porous feature strongly depends on discharging nature involved in MAO process [9]. However, with the further increase of time, the micro-pores on the surface seemed to be much less, and the coatings became much dense. The best treatment time is about 25 min for LY12 alloy to obtain the dense coatings.



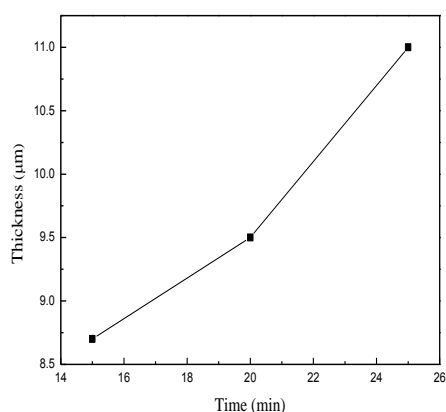
**Figure 4.** Surface morphologies of the ceramic coatings on LY12 alloy after different MAO treatment time. (a) 15 min, (b) 20 min, (c) 25 min.

Figure 5 shows the variation of the thickness of the MAO coatings on LY12 alloy as a function of oxidation time. With an increasing oxidation time, the thickness of the coatings increases rapidly. An approximately linear growth of the coatings was also observed. The growth rate of the coatings is very fast at the initial stage, and the coating thickness can reach 8.7 μm at 15 min. However, in the period of 20 to 25 min, the thickness only goes up from 9.6 to 11 μm.

XRD patterns of the MAO coatings on LY12 alloy are shown in Fig. 6 under different oxidation time. There are  $\gamma$ - $\text{Al}_2\text{O}_3$  and  $\alpha$ - $\text{Al}_2\text{O}_3$  in the MAO coatings, and the intensity of these diffraction peaks increases with an increasing time. Moreover, the peaks of aluminum substrate become to be weak when the thickness of the coatings increases. It has been indicated that the composition of the coatings may have a lot of  $\gamma$ - $\text{Al}_2\text{O}_3$  phase and a small amount of  $\alpha$ - $\text{Al}_2\text{O}_3$ . Obviously,  $\gamma$ - $\text{Al}_2\text{O}_3$  phase occurred initially and then transformed into  $\alpha$ - $\text{Al}_2\text{O}_3$  phase.

### 3.3 Cross sectional structure of MAO film on LY12 alloy

Fig. 7 shows the SEM micrographs of the cross-sections for the LY12 alloys subjected to the MAO treatment. It can be noted that the MAO coatings have a good adhesion with the alloy substrate. It was found that the coating/metal interface was not very clear, and the oxygen content increases rapidly at the interface. The thickness of the oxide coating is about 15 μm. The coating contains two layers, an outer porous layer and an inner barrier layer. In general, barrier layer have great influences on the



**Figure 5.** Variation of the thickness of MAO coatings on LY12 alloy with oxidation time.

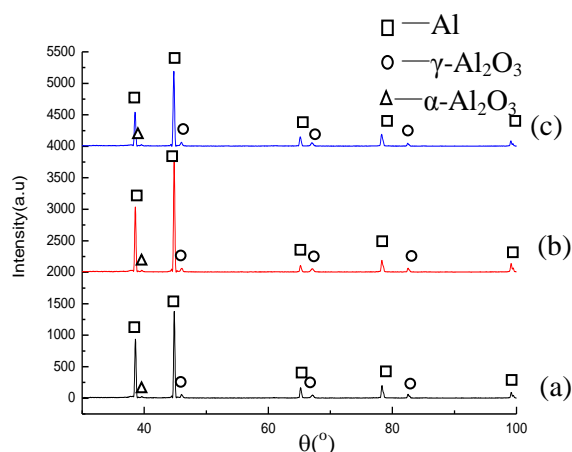


**Figure 6.** XRD patterns of MAO coatings on LY12 alloy. (a) 15 min, (b) 20 min, (c) 25 min.

corrosion barrier of MAO coatings [9]. With an increase in the thickness of the coating, the outer porous layer becomes much thinner, and the inner barrier layer will be thicker, which can account for a majority of coatings.

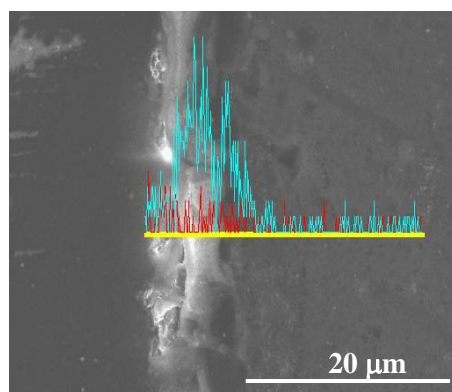


**Figure 7.** Back-scattered electron image of the cross-sectional MAO coating on LY12 alloy under a voltage of 480 V and an oxidation time of 25 min.

#### 4. Conclusions

The ceramic layers formed on the surface of the LY12 alloy has been obtained by different micro-arc oxidation treatment conditions. Different surface morphologies of MAO films were obtained under different conditions. The thickness of MAO coatings on the LY12 alloy increases with an increase of voltage and oxidation time. The MAO coatings contain two layers, an outer porous layer and an inner barrier layer. These films consist mainly of  $\gamma\text{-Al}_2\text{O}_3$  phase and a small amount of  $\alpha\text{-Al}_2\text{O}_3$  phase.

#### Acknowledgment

This work was supported by Shenyang Science & Technology Ministry (No.F15-200-6-03).

#### References

- [1] Wirtz G P, Brown S D and Kriven W M 1991 Mater. Manufac. Proc. **6** L87
- [2] Sundararajan G and Rama Krishna L 2003 Surf. Coat. Technol. **167** L269
- [3] Hoche H, Scheerer H, Broszeit E and Berger C 2003 Surf. Coat. Technol. **174-175** L1018
- [4] Yerokhin A L, Nie X and Leyland A 1999 Surf. Coat. Tech. **122** L 73
- [5] Yerokhin A L, Lyubimov V V and Ashitko R V 1999 Ceram. Int. **122** L 1
- [6] Kojima Y Mater. Sci. Forum 2000 **350/351** L3

- [7] Liang J, Guo B G, Tian J, Liu H W, Zhou J F and Xu T 2005 Appl. Surf. Sci. **252** L345
- [8] Gray J E and Luan B 2002 J. Alloys Compd. **336** L88
- [9] Cai Q Z, Wang L S, Wei B K and Liu Q X 2006 Surf. Coat. Technol. **200** L3727